σ

Journal of Engineering and Natural Sciences
Mühendislik ve Fen Bilimleri Dergisi

Sigma
2004/3

Invited Review Paper

STRUCTURAL AND OPTICAL PROPERTIES OF Si AND Ge NANOCRYSTALS EMBEDDED IN SiO_2 MATRIX BY ION IMPLANTATION

Raşit TURAN[*1], Uğur SERINCAN[1], Giray KARTOPU[2], Terje G. FINSTAD[3]

[1] Middle East Technical University, Department of Physics, Ankara-TURKEY
[2] De Montfort University, Faculty of Applied Sciences, The Gateway, Leicester, LE1 9BH, UK
[3] University of Oslo, P.O. Box 1048 Blindern, NO-0316 Oslo-NORWAY

Geliş/Received: 15.08.2004

ABSTRACT

It has been recently established that upon annealing at high temperatures impurity atoms implanted into SiO_2 matrix precipitate and form crystal islands with nanometer size. These nanostructures are expected to have interesting electrical and optical properties which can be utilized in the production of new opto- and micro-electronic devices. In this work, properties of Ge and Si nanocrystals formed in SiO_2 matrix by ion implantation followed by an annealing process were studied extensively. The formation of Ge nanocrystals was identified by Raman spectroscopy and Transmission Electron Microscopy. Ge islands with well defined spherical shapes were seen by the Transmission Electron Microscopy. The effects of process conditions such as the annealing time and temperature were studied. Evolution of Ge nanocrystal formation was clearly monitored and modeled by Raman sprectroscopy. Fourier Transform Infrared spectroscopy was employed to observe the structural variations in the SiO_2 matrix during the formation of both Si and Ge nanocrystals. Si nanocrystals were studied by Photoluminescence. Two broad emission bands in the yellow-orange and near-infrared regions of the light spectrum were recorded. The intensity of these bands depends on the duration and the temperature of the annealing process. These bands are attributed to transitions in defects or chain like Si formations and nanocrystals, respectively.
Keywords: Semiconductor nanocrystals, ion implantation, SiO_2

SiO_2 MATRİS İÇERİSİNE İYON EKME YÖNTEMİYLE YERLEŞTİRİLMİŞ Si VE Ge NANOKRİSTALLERİNİN YAPISAL VE OPTİKSEL ÖZELLİKLERİ

ÖZET

Son yıllarda, SiO_2 matris içerisine ekilmiş katkı atomları yüksek sıcaklıklarda fırınlandıklarında nanometre boyutunda kristal adacıklar oluşturdukları gösterilmiştir. Bu nanoyapıların ilgi çekici elektrik ve optik özelliklere sahip olması beklenmektedir ve böylece bu yapılar opto- ve mikro-elektronik aygıt yapımında değerlendirilebileceklerdir. Bu çalışmada, SiO_2 matris içinde iyon ekme ve takiben fırınlama yöntemiyle oluşturulan Ge ve Si nanokristallerinin özellikleri geniş çaplı çalışılmıştır. Ge nanokristallerinin oluşumu Raman spektroskopisi ve Geçirgenli Elektron Mikroskobu (TEM) yöntemleriyle çalışılmıştır. Ge adacıkları ve onların belirgin küresel şekilleri TEM yöntemiyle gözlenmiştir. Fırınlama süresi ve sıcaklığı gibi üretim koşullarının etkileri çalışılmıştır. Ge nanokristallerinin oluşum aşaması Raman spektroskopisi kullanılarak açık bir şekilde görüntülenmiş ve modellenmiştir. Si ve Ge nanokristallerinin oluşum aşamasında, SiO_2 matrisin yapısal değişmeleri FTIR spektroskopisiyle incelenmiştir. Si nanokristalleri fotoluminesans yöntemiyle çalışılmıştır. Sarı-turuncu ve yakın-kızılötesi bölgelerinde iki geniş ışıma tepesi kayıt edilmiştir. Bu tepelerin şiddetlerinin fırınlama süresi ve sıcaklığına bağlı olduğu gösterilmiştir. Bu tepelerden birincisi kusurlara veya zincir benzeri Si oluşumlarına, ikincisi ise nanokristallere atfedilmiştir.
Anahtar Sözcükler: Yarıiletken nanokristaller, iyon ekme, SiO_2

[*] Sorumlu Yazar/Corresponding Autor: e-mail:turanr@metu.edu.tr, Tel: (0312) 210 5069

1. INTRODUCTION

There has been much interest in synthesizing semiconductor nanocrystals (NCs) in silicon oxide (SiO_2) in the recent decade because of their optical [1-4] and electrical properties [5]. The recent activities in this field are motivated by the potential applications of semiconductor NCs in the fabrication of new opto- and micro-electronic devices. Several methods can be used to fabricate such structures [6-10]. Among these, ion implantation offers great flexibility in the NC formation by a control of process parameters, considerable freedom from thermodynamical limitations and extreme chemical purity. Recently, we have reported on the fabrication of Ge NCs ranging from 2 to 25 nm in size embedded in a SiO_2 matrix by using the ion implantation technique [11-13]. The formation mechanisms of Ge NCs have been discussed in these reports. We have also reported on the optical properties of Si NCs formed in SiO_2 [14].

NCs are clusters with the size of 1-100 nm formed either on a substrate or in a matrix of different materials. The production and characterization of NCs are important and sometimes challenging issues due to the difficulties in controlling and measuring the small quantities with nanometric dimensions. The technique of ion implantation provides an easy and compatible method in controlling the structural, optical and electrical properties of NCs. The formation of NCs by ion implantation is realized by introducing the accelerated atoms into a matrix, which is SiO_2 in the present case, and then annealing the sample at an elevated temperature which is high enough to induce the crystallization. Annealing process should be done in a controlled atmosphere in order to avoid the undesired effect of oxygen and contaminating species in air. The parameters of the ion implantation such as the ion energy (speed), ion dose, and the parameters of the annealing process such as the annealing temperature and duration determine the size and the distribution of the nanostructures formed. Understanding the physical and chemical processes that took place during the ion implantation and annealing are very important in achieving a reliable and reproducible methodology for the NC formation.

This paper presents a review of our recent works on various aspects of Si and Ge NCs formed in SiO_2 by ion implantation under various experimental conditions. High resolution Transmission Electron Microscopy (TEM), Photoluminescence (PL) spectroscopy, Raman spectroscopy (RS) and Fourier Transform Infrared (FTIR) spectroscopy have been used to characterize the structural, chemical and optical properties of the Si and Ge nanostructures.

2. EXPERIMENTAL PROCEDURES

SiO_2 films with thickness of 200 or 250 nm were prepared by standard wet thermal oxidation of p-type single (100) Si wafers with resistivities of 25-30 Ω cm. SiO_2 films were implanted with ^{74}Ge and ^{28}Si ions with doses in the range $3x10^{16}$ cm^{-2} – $1.5x10^{17}$ cm^{-2} at an energy of 100 keV using a 0-200 keV Varian DF4 implanter. Implanted films were annealed under N_2 atmosphere in a temperatures range of 700-1050 ^oC.

Samples for cross-sectional TEM were prepared using standard techniques. The structure of the different samples was examined at 200 keV using an analytical JEOL 2000 FX TEM and a field emission analytical JEOL 2010 F TEM equipped with a Noran Vantage DI+ energy dispersive X-ray spectroscopy (EDS) system. Raman scattering spectra of the films were obtained before and after annealing, in back-scattering configuration with a Renishaw RM series Raman microscope using a 514.5 nm Ar^+ laser excitation source. All of the measurements were carried out at room temperature, using a total laser power of either 4 or 0.4 mW (on the sample). The beam diameter was 1 m on the sample surface and scattered light was collected with a CCD camera on the head of the microscope. The spectral resolution was 1 cm^{-1}. FTIR spectroscopy were used in the absorbance mode (350-2500 cm^{-1}, 2 cm^{-1} resolution) to monitor the Si-O stretching peak, its intensity and full-width at half-maximum (FWHM). Samples were measured under the same experimental conditions for comparison. PL spectroscopy was performed by a

computer controlled Oriel MS257 monochromator with a back thinned Hamamatsu CCD camera. The samples were excited by a NdYag laser operating at 532 nm.

3. RESULTS AND DISCUSSIONS

3.1. Evolution and Characterization of Ge Nanocrystals Formed in SiO_2 Matrix

During the fabrication of Ge NCs by ion implantation and subsequent annealing, diffusion of the implanted Ge away from the regions with the highest Ge concentration towards the Si/SiO_2 interface can occur. This diffusion results in an accumulation of the implanted species at the Si/SiO_2 interface [13]. Although most of the implanted Ge will remain in a region around the projected range where Ge NCs are formed, a significant amount of the species can be located at the Si/SiO_2 interface after annealing as a result of this effect.

Figure 1 shows the TEM image of a sample implanted with $1x10^{17}$ cm^{-2} ^{74}Ge and annealed at 900 ^{o}C for 1 h. It can be clearly seen that, Ge NCs with well defined spherical shapes were formed. The crystallinity of the islands was identified by the selected area diffraction [12]. The size of the crystal islands can be determined from

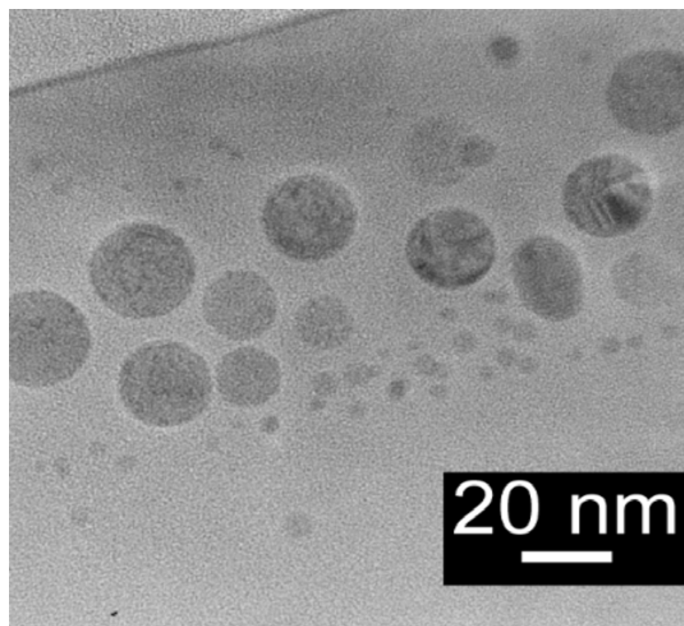

Figure 1. TEM image of a SiO_2 film implanted with a dose of $1x10^{17}$ cm^{-2} ^{74}Ge after annealing for 1 h at 900 °C under N_2

the TEM images even though the actual size might be larger than the apparent size which depends on where the NCs are cut during the preparation of cross-sectional samples. Bearing this uncertainty in mind, the NC sizes are estimated to vary in the of 2-25 nm. It is seen from the TEM picture that these NCs fall into two groups: Group1 with small NCs has an average grain size of 4 nm and the group 2 with large crystals has an average grain size of 20 nm. This can be understood by considering the growth and coarsening theory (i.e. Ostwald Ripening [15]) according to which some NCs grow while the others shrink. It was however observed that

the properties of these nanostructures are sensitive to the processing conditions. When the same sample is annealed at 1000 ^{o}C or above for 1h a dark band close to the surface and voids beneath this region were observed [12]. The dark region was determined to be GeO_x formed during the annealing. It was shown that Ge atoms left their position where the NC formed and then oxidized, resulting in the formation of a band of GeO_x layer and voids in the position of nanocrystalline islands.

Figure 2 shows the Raman spectra of the films implanted with $1x10^{17}$ cm^{-2} ^{74}Ge. The annealed film in this figure is similar to the one for which the TEM image was given in Fig. 1. The Raman spectrum of the as-implanted film (Fig. 2(a)) is similar to that of amorphous-Ge [16, 17]. In the case of disordered semiconductors, such as amorphous and nanocrystalline, the selection rule that determines the Raman spectra of the bulk crystals is either fully or partially violated (relaxed) so that phonons other than the zone-centered phonons can also be observed in their Raman spectra. On the other hand, the spectrum of the annealed film exhibits a sharp peak near 300 cm^{-1}, indicating the crystallization of Ge in the film. The width and spectral shape of this peak are different from those of bulk Ge but similar to those of nanocrystalline Ge [18]. In these measurements, the zone-centered Ge optical phonons peaked at 303.3 cm^{-1} with a FWHM of 7.0 cm^{-1} in the spectrum of bulk Ge (Fig. 2(c)); whereas the peak in the spectrum of nanocrystalline Ge (Fig. 2(b)) is downshifted to 301.5 cm^{-1} and asymmetrically broadened towards the lower frequency with respect to the bulk Ge peak.

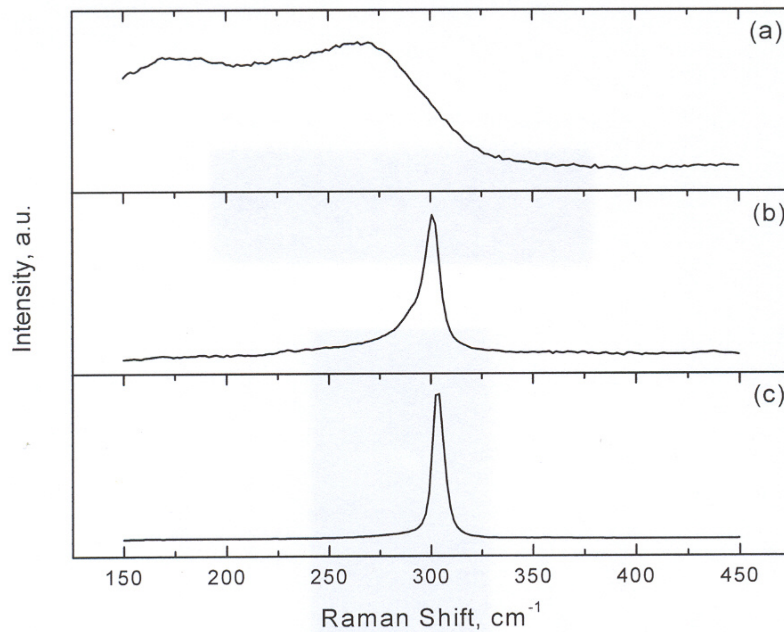

Figure 2. Raman spectra for a $1x10^{17}$ cm^{-2} ^{74}Ge-implanted SiO_2 film (a) before and (b) after annealing (at 900 ^{o}C for 45 min under N_2 atmosphere) and (c) bulk Ge

As we reported in a previous study [19], the Raman peak can be used to estimate the NC size and distribution by using a theoretical model developed specifically for such structures. For the background-subtracted optical phonon peak positioned at 300 cm^{-1}, a line shape fit is made as shown in Fig. 3 for $\overline{L}$ = 8.7 nm and σ = 2.1 nm. It can be

seen that the agreement of the line shape is fairly good. When compared with the TEM picture of the NCs grown in a similar sample (e.g. Fig. 1), we see that this value (8.7 nm) falls into the size range observed directly from the TEM picture. Keeping in mind that the Raman spectra change drastically when the mean crystallite size is below 20 nm, we can conclude that the effect of group 2 NCs with large crystals on the asymmetry of the Raman spectra is small. We confirmed this by using multiple size distribution functions in our calculations. In addition, we expect group 1 NCs to be larger and group 2 NCs to be smaller with respect to the sizes measured from the TEM image, since the annealing time was 15 min shorter for the Raman samples. We can thus confidently conclude that the average size of 8.7 nm calculated from the Raman spectrum is a good estimate of the average size of the NCs.

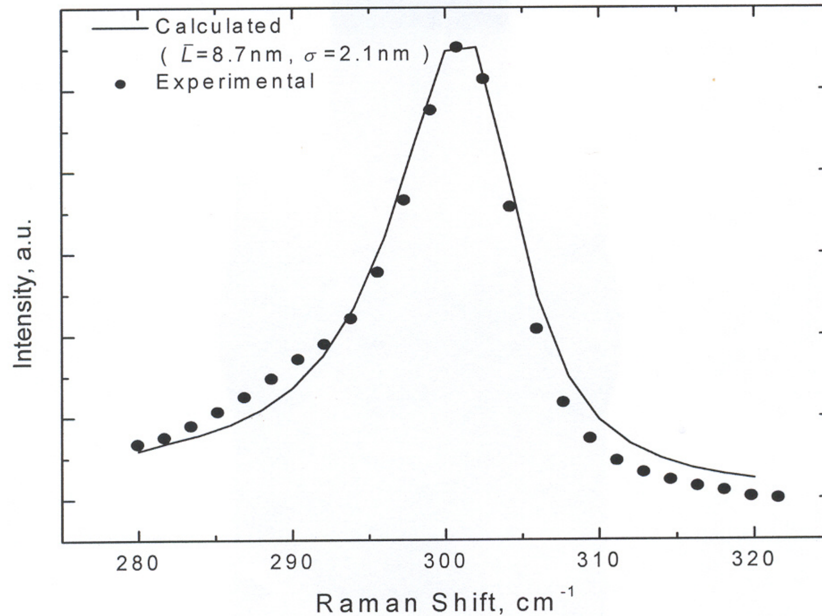

Figure 3. Experimental background-subtracted Raman spectrum of Ge NCs compared to theoretical Raman spectrum calculated for $\bar{L}$ = 8.7 nm and σ =2.1 nm using a phonon confinement model

3.2. Structural Variations in the SiO_2 Matrix During the Formation of Si and Ge Nanocrystals

FTIR spectra of Si and Ge implanted samples as a function of annealing temperature and a non-implanted oxide are shown in Figs. 4(a) and (b), respectively. A characteristic feature seen in these figures is the asymmetric shape of the Si-O-Si bond stretching vibration peak in the lower wavenumber part of the spectra. This asymmetric feature can be related to the presence of non-stoichiometric SiO_x with x<2. Tsu et al. [20] showed that the Si-O bond stretching vibration for SiO_x (x<2) occurs between 965 and 1060 cm^{-1}. The effect of ion implantation manifests itself as the formation of non-stoichiometric oxide with x<2. This is understandable because of two main effects of Si ion implantation into SiO_2: The introduction of excess Si into the matrix and the breaking Si-O bonds during slowing down of the implanted atoms. Upon annealing at sufficiently high temperature the deformed oxide bonds start to recover and excess Si atoms

precipitate to form NCs, leading to decrease in the shoulder seen in the low wavenumber side of the FTIR curve. In the case of Ge implanted sample, the same shoulder resulted from the deformation in the SiO_2 matrix is seen in the lower wavenumber side of the main peak. However, there are significant differences between the FTIR spectra of the Ge and Si implanted samples. A comparison of Figs. 4(a) and (b) reveals that the recovery of Si-O networks occurs at much lower temperatures in the case of the Ge implantation. This situation can be explained as follows: Excess Ge and Si atoms in the SiO_2 matrix deformed the Si-O bond structure by bonding with O or Si. For example in the case of Ge implantation, Si-O bonds were broken and some SiGe-O, Ge-Ge, Ge-O, Si-Si and Si-Ge and individual dangling bonds are formed [21]. During the annealing process, the excess Ge and Si atoms leave their initial positions and form clusters of a few nanometers. This segregation process is observed in the FTIR spectra as the reduction of the shoulder and recovery of the stoichiometry of the SiO_2 matrix as shown in Figs. 4(a) and (b). It is well known that Ge atoms are not soluble in SiO_2 and completely segregated out of the growing oxide if one oxidizes Si crystal containing Ge atoms [22]. This is due to the fact that the formation of SiO_2 is thermodynamically more favorable than the formation of GeO [23] and that the binding energy of the Si-O bonds (8.3 eV) is greater than that of Ge-O (6.8 eV). In addition to the precipitation in the matrix, we showed that some Ge atoms are segregated on the underlying Si substrate [13]. The rejection of Ge by the SiO_2 matrix leads to high diffusivity for Ge atoms, resulting in the formation of Ge NCs at low temperatures compared to Si NCs. This situation can also be perceived from the Fig. 5, where the intensity of the absorption peak of the spectra, normalized to the pure SiO_2 matrix, is plotted against the annealing temperature. The difference in the variation of peak intensity for Si and Ge implanted samples as a function of the annealing shows the same correlation with the Si and Ge NC formation in the SiO_2 matrix. In the case of Ge implanted sample, the signal intensity increases significantly at 800 ^{o}C and reaches almost the same value as that of the sample annealed at 1000 ^{o}C. This indicates again that Ge segregation form the SiO_2 matrix is completed at very low temperatures.

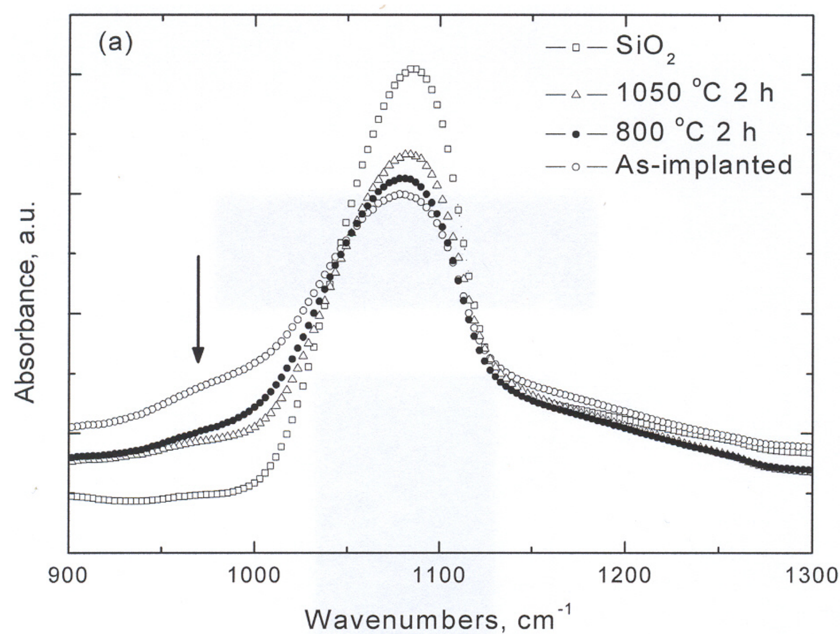

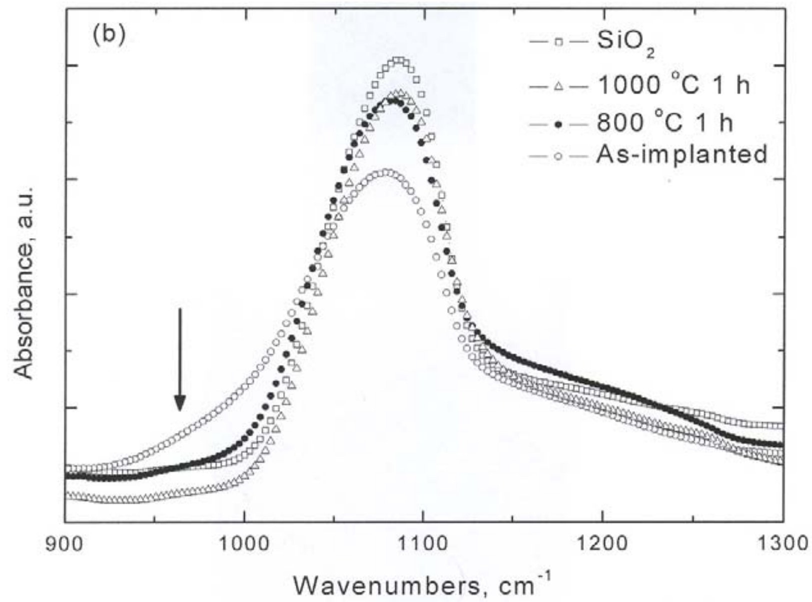

Figure 4. FTIR spectra of samples implanted at a dose of $1.5x10^{17}$ cm^{-2} at 100 keV with (a) ^{28}Si and (b) ^{74}Ge ions. Shoulder formation is indicated by arrow

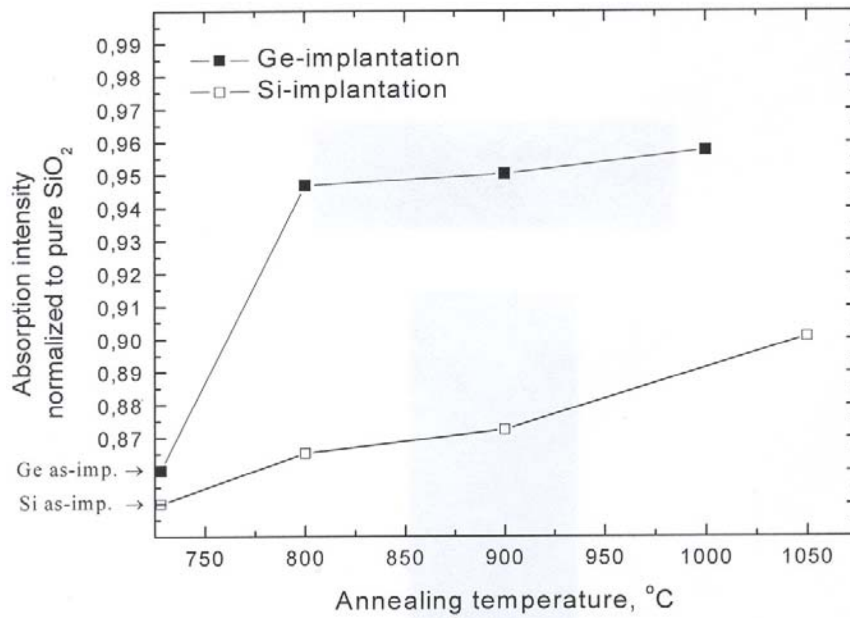

Figure 5. Annealing temperature dependence of absorption intensity of the Si-O stretching peak, obtained from Ge- and Si-implanted samples. For reference, the as-implanted values are indicated also

3.3. Optical Properties of Si Nanocrystals

Si NCs embedded in SiO_2 is a promising material system for the fabrication of Si-based light emitting devices. Light emitting properties of these structures are therefore the main concern of the studies in this field. Major experiments probing the light emission properties of NCs are based on the PL or Electroluminescence (EL) spectroscopy. It is now well established that SiO_2 matrix implanted with Si or Ge exhibits light emission in the blue/ultraviolet and red/infrared regions of the spectrum. The former emission band is usually connected to the defects formed in SiO_2 during ion implantation, and the latter one is related to the NCs. In the sample containing Ge NCs, we observed a wide emission band (not shown here) centered about 550 nm. We believe that this band is related to the lattice defects as observed by many other groups. Ge NCs did not show any observable light emission in the red/near- infrared region in our samples, probably due to the dominance of the non-radiative recombination of excited electron-hole pairs.

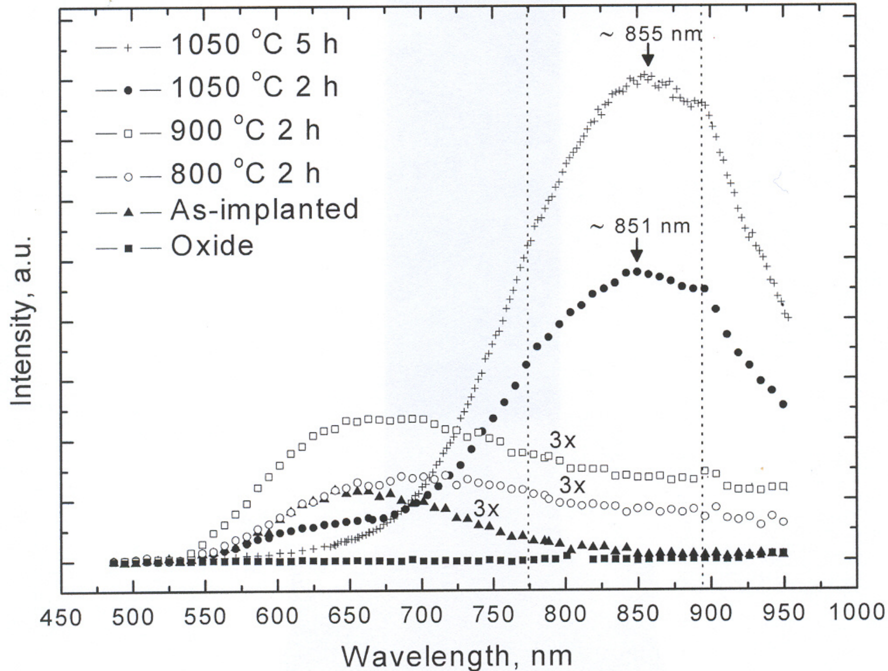

Figure 6. Room temperature PL of a sample which is implanted with ^{28}Si at a dose of $1.5x10^{17}$ cm^{-2} at 100 keV and annealed at various temperatures and times

In the case of Si NCs, strong light emission has been obtained in the range of 600-900 nm in agreement with other reported results. Figure 6 shows typical PL spectra measured from the Si implanted SiO_2 films annealed at different temperatures using a NdYag laser with a power of 300 mW. Samples were implanted with ^{28}Si at a dose of $1.5x10^{17}$ cm^{-2} and annealed at various temperatures for 2 or 5 h under N_2 atmosphere. For the as-implanted sample and samples annealed below 1050 °C a broad peak at ~ 650 nm is observed. By increasing the annealing temperature up to 1050 °C we observed that the intensity of this peak increases first and decreases later, while a new peak appears at ~ 850 nm which has two sub-peaks at ~ 775 and 900 nm. The emission is so strong that it can be seen by naked eye in a dark room. The increase in the PL intensity could be explained in terms of annealing of defects that can give rise to non-radiative

recombination. In addition, the increase in the annealing time at this temperature causes the peak at ~ 650 nm to disappear and the intensity of the peak at ~ 850 nm to increase. Same behavior in Si implanted samples was reported by Ghislotti et al. [24]. They attributed this peak to the defects like clusters or chain of silicon. This assumption was also confirmed by our etch experiment which will be discussed in the next section.

Comparison of the peak positions of samples annealed at 1050 ^{o}C for 2 and 5 h points that, the peak at ~ 850 nm shows a little redshift with increasing annealing time while the peaks at ~ 775 and 900 nm remains at the same position. The redshift is expected because the size of the NCs increases with annealing time and temperature and indicates that this peak results from the NCs. The sudden appearance of this peak at 1050 ^{o}C evidences also that the source of this peak is NCs. Since this temperature is closer to the melting temperature of bulk Si the formation of NCs is expected at this temperature.

3.4. Profiling the Illumination Centers by Controlled Etch Experiment

As we know from the calculated distribution of Si atoms after the ion implantation [14], Si concentration increases towards 140 nm from the surface and then decreases. NC formation is then expected to start in the region where the Si concentration is highest (140 nm). It is also expected and confirmed experimentally [25] that NCs with largest dimension are formed in this region. In order to see the correlation between the PL emission and the Si initial distribution, we have carried out an experiment in which PL spectra were taken while thin layers of SiO_2 layers were removed from the surface by etching with a buffered HF solution. Fig. 7 shows the variation of the PL spectrum and the peak position of the 850 nm peak as a function of etch depth. It is seen that the PL peak at ~ 850 nm shows a redshift in the first phase of the etching and blueshift afterwards down to a wavelength of 790 nm. This can be explained by considering the Si distribution and size dependent phenomenon: In the initial stages of the etching process, smaller NCs and the other formation of Si atoms (chains and/or clusters) are removed from the region close to the surface. The size of the NCs increases towards the projected range and the emission from these NCs becomes more effective as the etching process progresses. After the region beyond the projected range is reached, the effect of largest NCs lessens and the emission peak starts to shift to the opposite direction, i.e. towards smaller wavelength. This blue shift continues until the whole SiO_2 layer is removed. The variation in the intensity of the PL spectra might be related to the effectiveness of the emission centers. Another important result of this experiment is the behavior of the peak at ~ 650 nm. This peak disappears after etching a thin SiO_2 layer (~ 15 nm) from the surface, showing that emission centers of this peak are located in the region closer to the surface where Si concentration is less and the defect concentration is high. This peak is more likely to result from Si chains and clusters as suggested in [24].

4. CONCLUSION

Si and Ge NCs formed by the ion implantation have been studied by TEM, Raman, FTIR and PL spectroscopy. Ge NCs produced in the SiO_2 matrix by ion implantation were characterized by RS. It was shown that the lineshape and the asymmetry in the Raman peak can be described successfully by including the effect of size and size distribution of NCs. The formation of Ge and Si NCs in SiO_2 matrix was monitored by FTIR spectroscopy in an indirect way which is the recovery of Si-O networks. We have shown that the recovery process in Si-O networks is quite different in Ge and Si implanted samples and the deformation caused by Ge atoms in the SiO_2 matrix can be recovered by annealing the implanted samples at lower temperatures than that by Si atoms. Si implanted samples were examined by using PL spectroscopy and two broad PL bands were observed for the annealed samples. It was found that samples annealed at low and high temperatures exhibit a yellow-orange and near-infrared emission, respectively. These emission

bands have been attributed to two distinct sources: Defects such as clusters or chain of silicon atoms located near the surface and radiative recombination of quantum-confined excitons in the Si NCs. Finally, we verified by the etch experiment that the peaks observed in the yellow-orange and near-infrared regions are related with the defects and NCs, respectively.

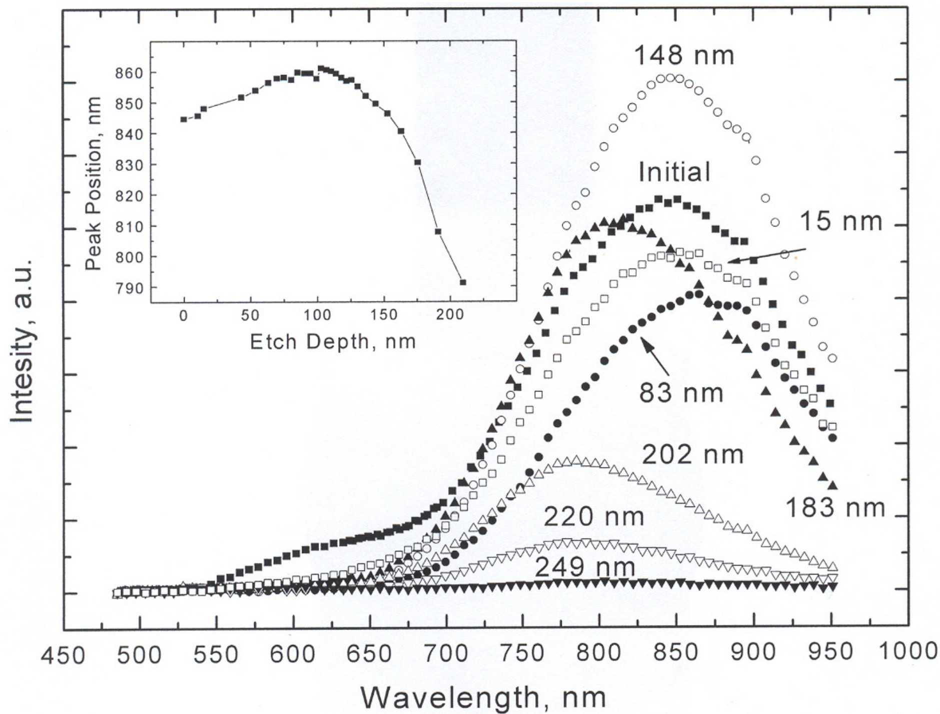

Figure 7. PL spectra of an etched sample which is implanted with Si at a dose of $1.5x10^{17}$ cm^{-2} at 100 keV and annealed at 1050 ^{o}C for 2 h under N_2 atmosphere. Corresponding etch depth (from the surface) values are indicated for each curve and PL peak position as a function of etch depth is designated in the inset

ACKNOWLEDGEMENTS

This work has been supported by Turkish Scientific and Technical Research Center (TUBITAK) and Norwegian Research Council (NFR).

REFERENCES

[1] Masuda., K, Yamamoto, M., Kanaya M., Kanemitsu, Y., (2002), "Fabrication of Ge nanocrystals in SiO_2 films by ion implantation: control of size and position", J. Non-Crystalline. Solids, Vol. 299-302, pp 1079-1083.

[2] Kanemitsu, Y., Uto, H., Masumoto, Y., Maeda, Y., (1992), "On the origin of visible photoluminescence in nanometer-size Ge crystallites", Appl. Phys. Lett., Vol. 61, No. 18, pp 2187-2189.

[3] Maeda, Y., Tsukamoto, N., Yazawa, Y., Kanemitsu, K., Masumoto, Y., (1992), “Visible photoluminescence of Ge microcrystals embedded in SiO_2 glassy matrices”, Appl. Phys. Lett., Vol. 59, No. 24, pp 3168-3170.

[4] Shcheglov, K. V., Yang, C. M., Vahala K. J., Atwater H. A., (1995), “Electroluminescence and photoluminescence of Ge-implanted Si/SiO_2/Si structures”, Appl. Phys. Lett., Vol. 66, pp 745-747.

[5] King, Y. C., King, T. J., and Hu, C., (2001), "Charge-trap memory device fabricated by oxidation of $Si_{1-x}Ge_x$", IEEE Trans. Electron. Devices, Vol. 48, No. 4, pp 696-700.

[6] Shimizu-Iwayama, T., Ohshima, M., Niimi, T. et al., (1993), “Visible photoluminescence related to Si precipitates in Si^+-implanted SiO_2”, J. Phys.: Condens. Matter, Vol. 5, No. 31, pp L375-380.

[7] Nogami, M., Abe, Y., (1994), “Sol-gel method for synthesizing visible photoluminescent nanosized Ge-crystal-doped silica glasses”, Appl. Phys. Lett., Vol. 65, No. 20, pp 2545-2547.

[8] Craciun, V., Boulmer-Leborgne, C., Nicholls, E. J., Boyd, I. W., (1996), “Light emission from germanium nanoparticles formed by ultraviolet assisted oxidation of silicon-germanium”, Appl. Phys. Lett., Vol. 69, No. 11, pp 1506-1508.

[9] Paine, D. C., Caragianis, C., Kim, T. Y., Shigesato, Y., Ishahara, T., (1993), “Visible photoluminescence from nanocrystalline Ge formed by H_2 reduction of $Si_{0.6}Ge_{0.4}O_2$”, Appl. Phys. Lett., Vol. 62, No. 22, pp 2842-2844.

[10] Hayashi, R., Yamamoto, M., Tsunetomo, K., Kohno, K., Osaka, Y., Nasu, H., (1990), ”Preparation and Properties of Ge Microcrystals Embedded in SiO_2 Glass Films”, Jpn. J. Appl. Phys., Vol. 29, No. 4, pp 756-759.

[11] Marstein, E. S., Gunnæs, A. E., Serincan, U., Turan, R., Olsen, A., and Finstad, T. G., (2002), “Nanocrystal and nanocluster formation and oxidation in annealed Ge-implanted SiO_2 films”, Surf. Coatings Technol., Vol. 158, pp 544-547.

[12] Marstein, E. S., Gunnæs, A. E., Serincan, U., Jørgensen, S., Turan, R., Olsen, A., and Finstad, T. G., (2003), “Mechanisms of void formation in Ge implanted SiO_2 films”, Nucl. Instr. and Meth. B, Vol. 207, No.4, pp 424-433.

[13] Marstein, E. S., Gunnæs, A. E., Turan, R., Olsen, A., Finstad, T. G. , and Serincan, U., “Introduction of interface states by Ge accumulation at the Si-SiO_2 interface by annealing Ge implanted SiO_2 films”, J. Appl. Phys., (at press).

[14] Serincan, U., Aygun, G. and Turan, R., “Selective Excitation and Depth Profiling of Light Emitting Centers in Si Implanted SiO_2”, submitted to J. Lumin.

[15] Verhoeven, J. D., (1975), Fundamentals of Physical Metallurgy, John Wiley & Sons, Inc., p. 400.

[16] Czachor, A., (1985), “Locator study of neutron and light inelastic scattering and infrared absorption in disordered solids”, Phys. Rev. B, Vol. 32, No. 9, pp 5628-5631.

[17] Bermejo, D. and Cardona, M., (1979), “Raman scattering in pure and hydrogenated amorphous germanium and silicon”, J. Non-Cryst. Solids, Vol. 32, No. 1-3, pp 405-419.

[18] Fujii, M., Hayashi, S., and Yamamoto, K., (1990), “Raman scattering from quantum dots of Ge embedded in SiO_2 thin films”, Appl. Phys. Lett., Vol. 57, No. 25, pp 2692-2694; Fujii, M., Hayashi, S., and Yamamoto, K., (1991), ” Growth of Ge Microcrystals in SiO_2 Thin Film Matrices: A Raman and Electron Microscopic Study”, Jpn. J. Appl. Phys., Vol. 30, No. 4, pp 687-694.

[19] Serincan, U., Kartopu, G., Guennes, A. E., Finstad, T. G., Turan, R., Ekinci, Y., and Bayliss, S. C., (2004), ” Characterization of Ge nanocrystals embedded in SiO_2 by Raman spectroscopy”, Semicond. Sci. Technol., Vol. 19, No. 2, pp 247-251.

[20] Tsu, D. V., Lucovsky, G. and Davidson B. N., (1989), “Effects of the nearest neighbors and the alloy matrix on SiH stretching vibrations in the amorphous SiO_r:H ($0<r<2$) alloy system”, Phys. Rev. B, Vol. 40, No. 3, pp 1795-1805.

[21] Yamamoto, M., Koshikawa, T., Yasue, T., Harima, H. and Kajiyama, K., (2000), "Formation of size controlled Ge nanocrystals in SiO_2 matrix by ion implantation and annealing", Thin Solid Films, Vol. 369, pp 100.

[22] Turan, R. and Finstand, T. G., (1992), "Electrical properties of Ge-implanted and oxidized Si", Semicond. Sci. Technol., Vol. 7, pp 75-81.

[23] Margalit, S., Bar-lev, A., Kuper, A. B., Aharoni, H. and Neugroschel, A., (1972), "Oxidation of silicon-germanium alloys", J. Cryst. Growth., Vol. 17, pp. 288.

[24] Ghislotti, G., Nielsen, B., Asoka-Kumar, P., Lynn, K. G., Gambhir, A., Di Mauro, L. F. and Bottani, C. E., (1996)," Effect of different preparation conditions on light emission from silicon implanted SiO_2 layers", J. Appl. Phys., Vol. 79, No.11, pp 8660-8663.

[25] B. Garrido, M. López, A. Pérez-Rodríguez, C. García, P. Pellegrino, R. Ferré, J. A. Moreno, J. R. Morante, C. Bonafos, M. Carrada, A. Claverie, J. de la Torre, A. Souifi, (2004), "Optical and electrical properties of Si-nanocrystals ion beam synthesized in SiO_2", Nucl. Instrum. Meth. B, Vol. 216, pp 213-221.